

The liquid–glass transition in sugars: Relaxation dynamics in trehalose

Herman Z. Cummins^{a,*}, Hepeng Zhang^{a,1}, Jiyoung Oh^b,
Jeong-Ah Seo^b, Hyung Kook Kim^b, Yoon-Hwae Hwang^b,
Y.S. Yang^c, Yun Sik Yu^d, Yongwoo Inn^e

^a Department of Physics, City College of CUNY, New York, NY 10031, United States

^b Research Center for Dielectric and Advanced Matter Physics and Department of Physics,
Pusan National University, Busan 609-735, South Korea

^c Institute of Nanoscience and Technology, Pusan National University, Busan 609-735, South Korea

^d Department of Physics, Donggeui University, Busan, South Korea

^e Department of Chemical Engineering, City College of CUNY, New York, NY 10031, United States

Available online 29 September 2006

Abstract

The liquid–glass transition in the disaccharide sugar trehalose mixed with small amounts of water was studied with calorimetry, photon correlation spectroscopy, Brillouin scattering, dielectric spectroscopy, and rheology measurements. Trehalose is of particular interest among the sugars because of its importance in biology, biochemistry, and the pharmaceutical industry, due to its ability to protect organisms, proteins, or membranes during dehydration (anhydrobiosis). Preliminary results of these experiments are presented and compared with each other and with previously published data on this material.

© 2006 Elsevier B.V. All rights reserved.

PACS: 81.05.Kf; 06.60.Ei; 65.60.+a; 78.35.+c

Keywords: Brillouin scattering; Dielectric properties; Relaxation, electric modulus; Glass transition; Calorimetry; Rheology; Structural relaxation

1. Introduction

Studies of the liquid–glass transition in glassforming molecular liquids such as orthoterphenyl, propylene carbonate, glycerol, salol, and metatoluidine with a variety of experimental techniques have been used extensively to test theories of the liquid–glass transition. One group of molecular glassforming materials that has received relatively little attention is the sugars, a subset of the carbohydrates. These include the monosaccharides (glucose, sorbose, mannose, galactose, and fructose), the disaccha-

rides (sucrose, lactose, maltose, and trehalose), and various higher polysaccharides. The structure of two important monosaccharides, glucose and fructose, and two important disaccharides, sucrose and trehalose, are shown in Fig. 1 [1]. Glucose, the body's main energy source, can exist in either the chain or ring form. Sucrose is composed of one glucose ring and one fructose ring, while trehalose contains two linked glucose rings. There have been many calorimetric studies of sugars designed to determine their glass-transition temperatures T_G [2–8], but there have been relatively few studies of the dynamics of either the liquid or glassy states of these materials.

The glass transition in sugars is important for several reasons. First, although water is obviously necessary for life, some organisms are able to withstand very low temperatures (cryopreservation) or to survive almost complete

* Corresponding author. Tel.: +212 650 6921; fax: +212 650 6923.

E-mail address: cummins@sci.cuny.cuny.edu (H.Z. Cummins).

¹ Present address: Center for Nonlinear Dynamics, University of Texas at Austin, Austin, TX 78712-0264, United States.

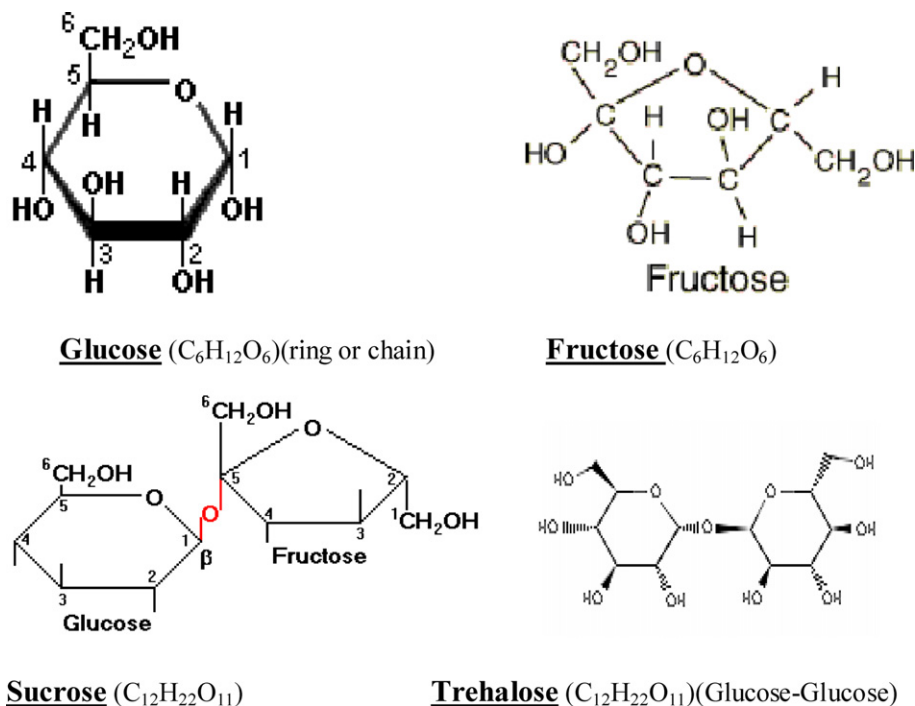


Fig. 1. Molecular structure of two monosaccharides glucose and fructose ($C_6H_{12}O_6$) and two disaccharides sucrose and trehalose ($C_{12}H_{22}O_{11}$). (Source <http://webbook.nist.gov/chemistry>).

dehydration (anhydrobiosis), even when 99% of their water content is removed, because they contain large amounts of sucrose or trehalose and can become reversibly glassy. This includes common organisms such as plants, yeast cells, and fungal spores, as well as microscopic animals such as nematodes, rotifers, and the cysts of brine shrimp. Some of these dried organisms may remain in this state for decades under favorable conditions until water becomes available. When that happens, they swell and resume the active state [9–13]. According to Elbein et al. [10], ‘This sugar (trehalose) is present in a wide variety of organisms, including bacteria, yeast, fungi, insects, invertebrates, and lower and higher plants, where it may serve as a source of energy and carbon. In addition, it has been shown that trehalose can protect proteins and cellular membranes from inactivation or denaturation caused by a variety of stress conditions, including desiccation, dehydration, heat, cold, and oxidation.’

Second, biochemists frequently suspend biomaterials such as proteins or membrane vesicles in aqueous solutions of disaccharides and then remove water by evaporation or freeze-drying to immobilize the biomaterial in a glassy matrix for spectroscopic study [14–20]. Trehalose is particularly efficient for this application since its T_G is above room temperature for residual water concentrations below ~10%. Cicerone and Soles [21] note that preservation of biological agents in nominally dry carbohydrate glasses has become increasingly important in the pharmaceutical and tissue engineering industries which rely on the ability to deliver functional proteins in the dry state. They have carried out elastic and inelastic incoherent neutron scatter-

ing studies of a series of trehalose glasses diluted with different amounts of glycerol. Their results indicate that short-wavelength high-frequency fluctuations are suppressed in these glasses and that this suppression is important to the stabilization of proteins in these glasses [21]. This suppression has also been found in molecular dynamics simulations [22]. Raman and neutron scattering studies of lysozyme dissolved in glycerol and trehalose have shown that the protein dynamics follow those of the solvent [23]. Another possible clue to the special properties of trehalose is suggested by molecular dynamics simulations by Lerbret et al. which indicate that trehalose binds to more surrounding water molecules than other disaccharides [24]. Possible mechanisms for the ability of trehalose to protect proteins against denaturation and to stabilize cell membranes were discussed in 1992 by Levine and Slade [25].

Third, the glass transition in sugars is important in the food industry [2–4]. Some familiar sugar-containing foods such as hard candy are prepared in the glassy state by boiling a water solution of sucrose and glucose (cane sugar and corn syrup) until the glass transition temperature is above room temperature. An illustrated elementary discussion of sugar glass and candy making can be found on the website of the Exploratorium [26]. Sugars also contribute to the long-term stability of foods as well as of biomaterials [27]. Also, since T_G for many sugars is above room temperature, experiments on aging effects can be carried out on sugars without cryogenic equipment, facilitating rapid temperature quenches. The drawbacks of spectroscopic studies of the glass-transition in sugars is that they are relatively weak light scatterers, and it is difficult to prepare dust-free samples.

We have undertaken studies of a number of sugars and sugar mixtures including glucose, maltose, galactose, fructose, sucrose, ribose, trehalose, glucose/sucrose, sucrose/trehalose, trehalose/maltose, sucrose/fructose (candy glass), and fructose/glucose using calorimetry (DTA and DSC), photon correlation spectroscopy, Brillouin scattering, dielectric spectroscopy, rheology, and X-ray diffraction, carried out in New York and Busan as part of a US–Korea collaborative research project. The results of some of these studies are being reported separately [28,29]. In this communication, we present a preliminary report of our experiments on trehalose.

Previous studies of the dynamical properties of trehalose include neutron scattering [21,30,31], Raman scattering [32], dielectric and infrared spectroscopy [33], dynamical mechanical analysis [34], and molecular dynamics studies [35].

2. Experimental

Trehalose dihydrate (Pharma grade 99.99%, lot 1H061) was generously provided by Cargill Inc., Minneapolis, MN. (trehalose dihydrate contains 9.53% water by weight). Anhydrous trehalose ($C_{12}H_{22}O_{11}$, mw 342.31, mp 97 °C) is a disaccharide composed of two linked glucose rings. The glass transition temperature T_G of anhydrous trehalose is ~ 114 °C [17]. It is well suited for optical studies since it is nonreducing and remains optically clear at relatively high temperatures where many other sugars become discolored.

Samples of molecular liquids for light-scattering experiments are usually prepared by vacuum distillation. For sugars, however, this method is not possible since dissociation (or caramelization) occurs at relatively low temperatures. Simply melting sugar samples is also not appropriate since the resulting melts are invariably dusty. We therefore prepared samples by dissolving the trehalose dihydrate powder in hot purified water to make a solution of typically $\sim 30\%$ sugar concentration. The solution was then filtered at room temperature with a syringe fitted with a Millipore 0.1 μm millex filter to remove dust. The filtrate was then either heated in a Sartorius model MA100C moisture analyzer, or else placed in a beaker with a teflon-coated magnetic stir bar and boiled slowly on a stirring hot plate to remove water. The boiling temperature was measured continuously during this procedure with a thermocouple thermometer. T_B increases as the volume decreases, slowly at first and then faster as the residual water content decreases. When the desired final boiling temperature was reached, the sample was removed from the hotplate, weighed to estimate the final water concentration, and poured into sample cells.

For light scattering (Brillouin scattering or Photon Correlation Spectroscopy) experiments, the sample cells were glass cylinders 16 mm in diameter and 16 mm high. After filling, the cell was sealed with a plastic stopper and teflon tape. It was then installed in a copper enclosure attached to

the cold finger of an Oxford DN1754 variable temperature LN2 cryostat. The temperature inside the cryostat was controlled by an Oxford ITC4 temperature controller with a Pt resistance thermometer. For the experiments described below, the typical boiling temperature was 126 °C, corresponding to a final water concentration of $\sim 9\%$ and a glass-transition temperature $T_G \sim 30$ °C.

2.1. Calibration

To prepare samples using the boiling method, we need to know both the residual water concentration $C(\text{H}_2\text{O})$ and the glass transition temperature T_G as functions of the boiling temperature T_B . To determine the relation between $C(\text{H}_2\text{O})$ and T_B , we carried out a calibration experiment in which 420 gm of unfiltered 30% Trehalose solution was put in a tall 500 ml glass container placed on a stirring hot plate. A chromel–alumel thermocouple probe (Omega type K) was immersed in the liquid and monitored with an Omega type 2175A digital thermometer. As boiling proceeded, the container was periodically removed from the hot plate and weighed. In the top panel (a) of Fig. 2, we show the measured water concentration vs. boiling temperature data (points). The solid curve is the result of fitting the data to the arbitrarily selected 4-parameter KWW function that was chosen because it provided a good fit to the data:

$$C(T) = b_1 \exp[-((T_B - b_2)/b_3)^{b_4}], \quad (1)$$

which gave: $b_1 = 1.236$, $b_2 = 100.29$, $b_3 = 2.419$, $b_4 = 0.412$.

The dependence of the glass transition temperature T_G on residual water concentration $C(\text{H}_2\text{O})$ has been discussed in several publications. Chen [19] reviewed the extensive trehalose literature in 2000. His Fig. 1 shows the various published values for $T_G(C)$ and indicates his choice for the optimum glass transition curve. (C is the residual water content; $C = 0$ represents pure anhydrous trehalose.) Several points from this curve are shown in the middle panel (b) of Fig. 2.

Chen [19] also reviewed various empirical fitting functions that have been used to fit the glass transition curve. Crowe et al. [17] reported an empirical fit to their Trehalose $T_G(C)$ data:

$$T_G(C) = 115.5 + 202.5C - 405.6C^{0.5}.$$

This equation is shown by a broken line in the middle panel (b) of Fig. 2. To improve the agreement with the glass transition curve of Chen et al., we refit this equation to the data points with the three numerical coefficients free and obtained the result indicated by the solid curve:

$$T_G(C) = 165.6 + 241.9C - 524.2C^{0.5}. \quad (2)$$

While this choice gives too high a value for T_G of anhydrous trehalose, it gives an excellent fit in the range of interest for our experiments.

Finally, combining the results for $C(T_B)$ (Eq. (1)) and $T_G(C)$ [Eq. (2)], we obtained the curve for T_G vs. T_B shown

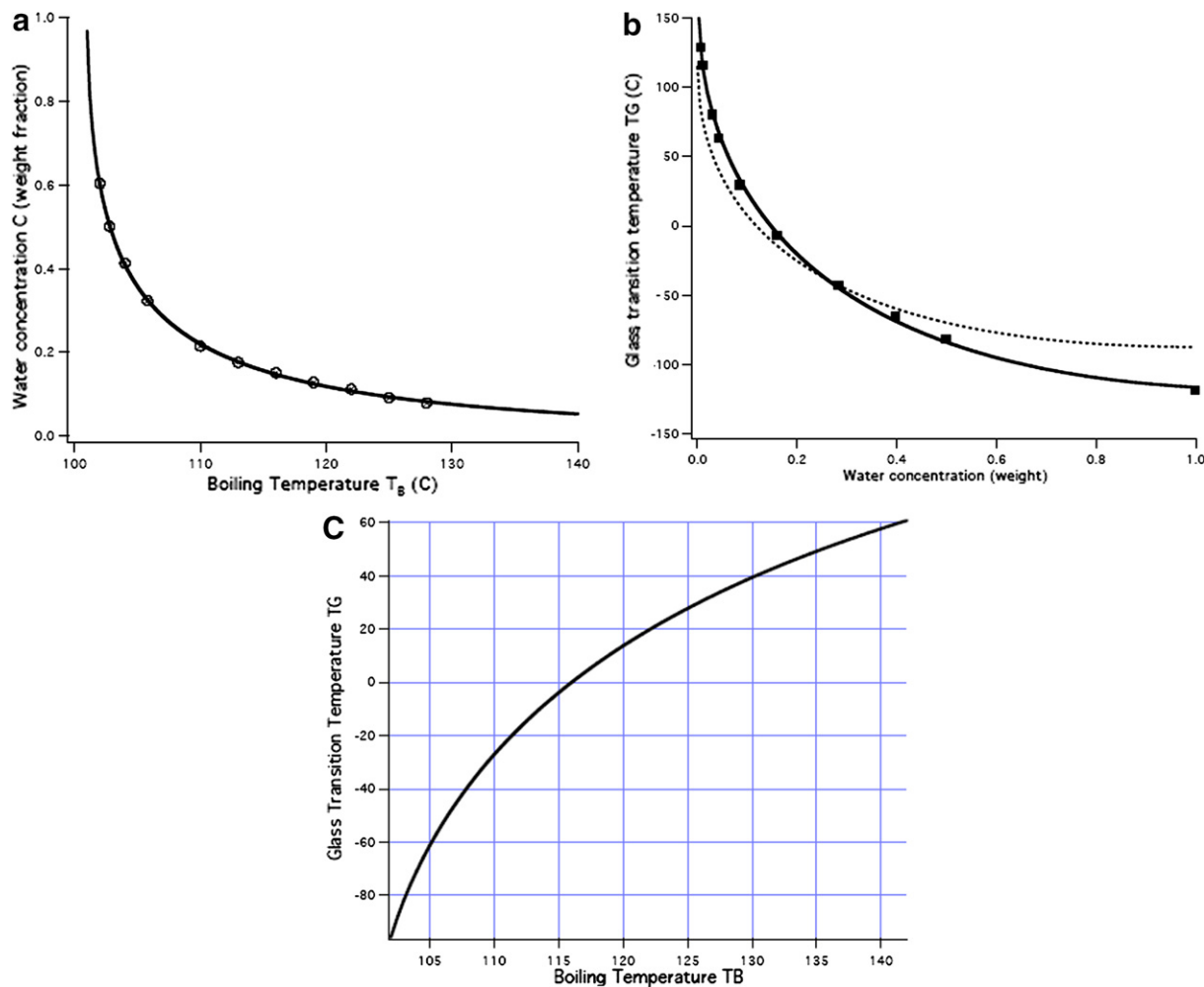


Fig. 2. (a) Water concentration (by weight) vs. boiling temperature T_B for aqueous trehalose solutions, (b) Glass transition temperature T_G vs. water concentration (from [19]). The lines are empirical fits discussed in the text, (c) T_G vs. T_B from the fits shown in (a) and (b).

in the bottom panel (c) of Fig. 2. Given the uncertainty in the glass transition curve, we assign an uncertainty of ± 5 °C to this result. For a sample prepared by boiling at 126 °C, the predicted glass transition temperature would therefore be $T_G = 30 \pm 5$ °C.

3. Results

3.1. Brillouin scattering

Brillouin scattering experiments were carried out to estimate T_G , since the Brillouin shift vs. temperature plot usually shows a distinct change in slope at T_G . This procedure was used recently, together with DSC measurements, to estimate T_G in a series of glucose/water mixtures [29]. The trehalose/water sample was prepared by boiling a filtered trehalose solution as described above, with a final boiling temperature of 123 °C. Brillouin spectra at $\theta = 90^\circ$ were obtained with single-mode 488 nm excitation and a Sandercock tandem Fabry–Perot interferometer. Spectra were collected at nine temperatures between 295 K and 345 K. The Brillouin lines were fit with a

damped harmonic oscillator function to find the Brillouin shift and width. The Stokes Brillouin components for four temperatures are plotted with the corresponding damped oscillator fits in Fig. 3. The measured Brillouin shifts and linewidths are plotted in Fig. 4. The slope of the Brillouin shift vs. temperature plot changes around 310 K (37 °C) indicating a glass transition at $T_G \sim 37$ °C, about 12 °C above the predicted value from Fig. 2 of 24 ± 5 °C.

3.2. Calorimetry

Differential scanning calorimetry (DSC) experiments provide a convenient way to estimate T_G due to the step-like increase in specific heat in the liquid relative to the glass, associated with the larger configurational entropy of the liquid. Various methods of estimating T_G from DSC data have been described; we will use the midpoint of the step in the DSC heating curves, although this tends to give a somewhat high value for T_G .

A Trehalose sample was prepared following the boiling procedure described previously with a final boiling temperature of ~ 125 °C and a final water concentration of 6%.

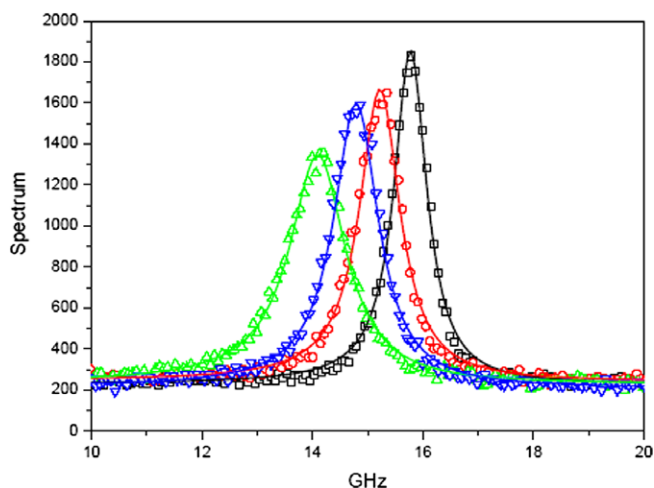


Fig. 3. Trehalose/10%water Brillouin spectra at $T = 295, 315, 325,$ and 345 K (right to left) with damped oscillator fits.

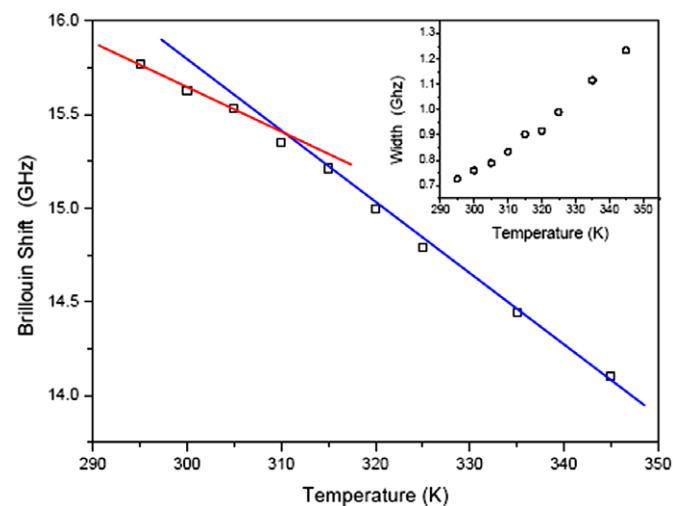


Fig. 4. Brillouin shifts from the fits in Fig. 3 vs. temperature. The change in slope at $T \sim 310$ K indicates the location of the glass transition temperature T_G . Inset: temperature dependence of the Brillouin linewidth.

DSC measurements were performed with a MAC Science model DSC3100 calorimeter at heating rates of 4, 5, 6, and 8 °C/min. The data are shown in Fig. 5. Taking T_G as the mid-point temperatures of the steps in these curves gave $T_G = 34.1, 35.1, 36.1,$ and 37.9 °C respectively, in reasonable agreement with – but somewhat higher than – the predicted $T_G = 28 \pm 5$ °C and close to the results obtained from the Brillouin scattering experiments.

Moynihan et al. [36] proposed that the dependence of the glass transition temperature T_G on the heating rate q is given by

$$d \ln |q| / d(1/T_G) = -\Delta h^* / R \quad (3)$$

(in units of K), where Δh^* is the activation enthalpy. They showed that Eq. (3) (in an equivalent form) holds for three glasses: As_2Se_3 , B_2O_3 , and $23\%K_2O-77\%SiO_2$. The corre-

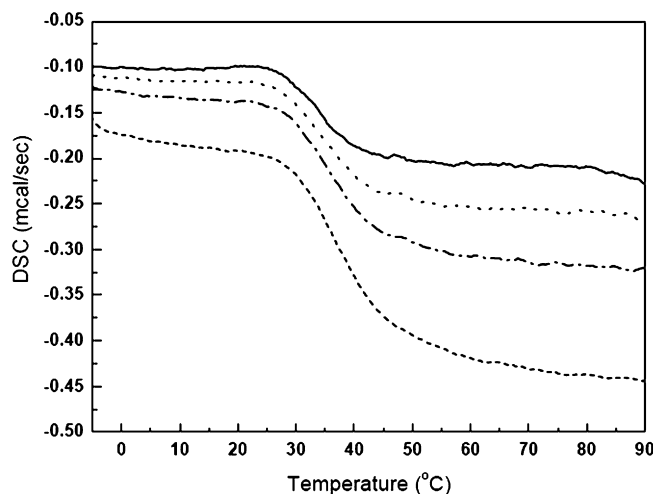


Fig. 5. Differential scanning calorimetry runs on a trehalose sample with 6% residual water concentration. Heating rates (top to bottom) are 4, 5, 6, and 8 °C/min. The corresponding glass transition temperatures, taken as the midpoint of the step in the heating curves, are 34.1, 35.1, 36.1, and 37.9 °C respectively.

sponding values found for Δh^* were 70, 92, and 101 kcal/mol., respectively.

For our trehalose/6% water data, a linear fit to the four data points gave $d \ln |q| / d(1/T_G) = -1.704 \times 10^4$ K, from which Eq. (3) gives $\Delta h^* = 33.9$ kcal/mol., comparable to but somewhat smaller than Δh^* for the three materials discussed in [36]. The strength of the heating rate dependence of T_G , as indicated by the increase in T_G when the heating rate is doubled, is 3.8 K in trehalose/6% water, comparable to the other three materials for which doubling of the heating (or cooling) rates increases T_G by 4.2, 4.8, and 8.8 K respectively.

3.3. Dielectric susceptibility

Frequency-dependent dielectric constant measurements at different temperatures were carried out using a cylindrical sample cell with inner and outer diameters of 6.8 mm and 8.7 mm, and height of 8.7 mm. Temperature was controlled with a PID controller. Two different measurement approaches were employed depending on the frequency range under consideration. For the frequency range of 0.1 Hz to 10 kHz, the in-phase and out-of-phase currents through the capacitor were measured using a Dual Phase Lock-in Amplifier (Stanford SR 830, USA) in conjunction with a Universal Waveform Generator (195 Wavetek/Datron, USA). For the frequency range of 100 Hz to 10 MHz, an Impedance Analyzer (HP 4194A, Hewlett-Packard USA) with a standard four-terminal pair configuration was used to measure the capacitance and conductance of the sample. The data obtained from the two methods were in excellent agreement where they overlapped.

In a dielectric study of glucose/water solutions, to be described in another publication, strong α -relaxation peaks

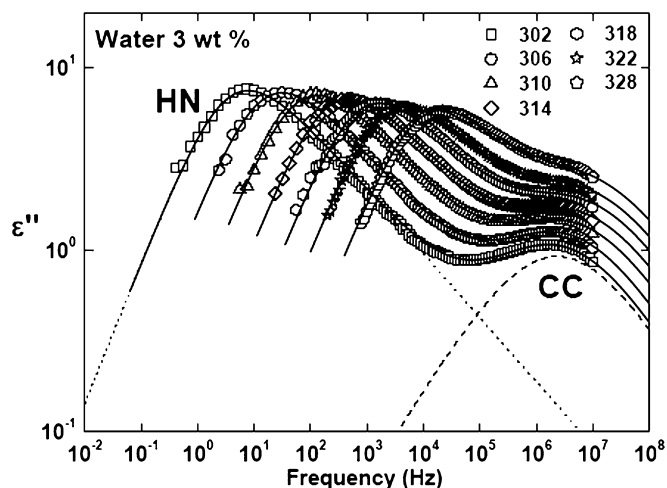


Fig. 6. Dielectric loss spectra $\varepsilon''(\omega)$ of glucose/3% water at $T = 302, 306, 310, 318, 322,$ and 326 K with fits to the sum of HN and CC functions.

were observed together with secondary relaxation structure, similar to the observations of Moran et al., [28]. Fig. 6 shows a series of dielectric $\varepsilon''(\omega)$ spectra for glucose with 3% by weight residual water concentration at five temperatures between 302 and 326 K. Fits to the sum of a Havriliak–Negami and Cole–Cole functions are also shown. In contrast to glucose, the trehalose/water samples did not exhibit α -relaxation peaks. In the low frequency region of the $\varepsilon''(\omega)$ spectra (10^{-2} – 10^4 Hz) there is a typical dc conductivity contribution with power-law dependence of $\varepsilon''(\omega)$ on ω as seen in Fig. 7(a). Attempts to remove this component by purification of the sample or subtraction of the dc conductivity failed to reveal any underlying α peaks, as shown in Fig. 7(b). The absence of α peaks indicates that in Trehalose/water solutions, α -relaxation is masked by the dc conductivity. De Gussemé et al. reported a similar result in their dielectric studies of anhydrous trehalose [33].

In Fig. 8 we show both the real and imaginary parts of $\varepsilon(\omega)$ at (a) $T = 40$ °C and (b) $T = 80$ °C. The secondary relaxation structure is seen to move to higher frequencies with increasing T , with its peak at ~ 4 MHz at $T = 40$ °C and at ~ 8 MHz at $T = 80$ °C.

3.4. Photon correlation spectroscopy

PCS data was obtained using a Brookhaven Instruments BI9000 digital correlator with logarithmic time base in cross-correlation mode. The excitation was ~ 125 mW of 4880 light from a single-mode Coherent Innova Argon laser. Data was collected for either 10 or 20 min in 400 channels with delay times between 100 ns and 20 s. Correlation data, normalized to the theoretical baseline, were fitted to a KWW function:

$$C(\tau) = b + a * \exp[-(t/\tau)^\beta]. \quad (4)$$

The baseline b for the fit was kept free along with τ , β , and the amplitude a , because the observed effective baseline was

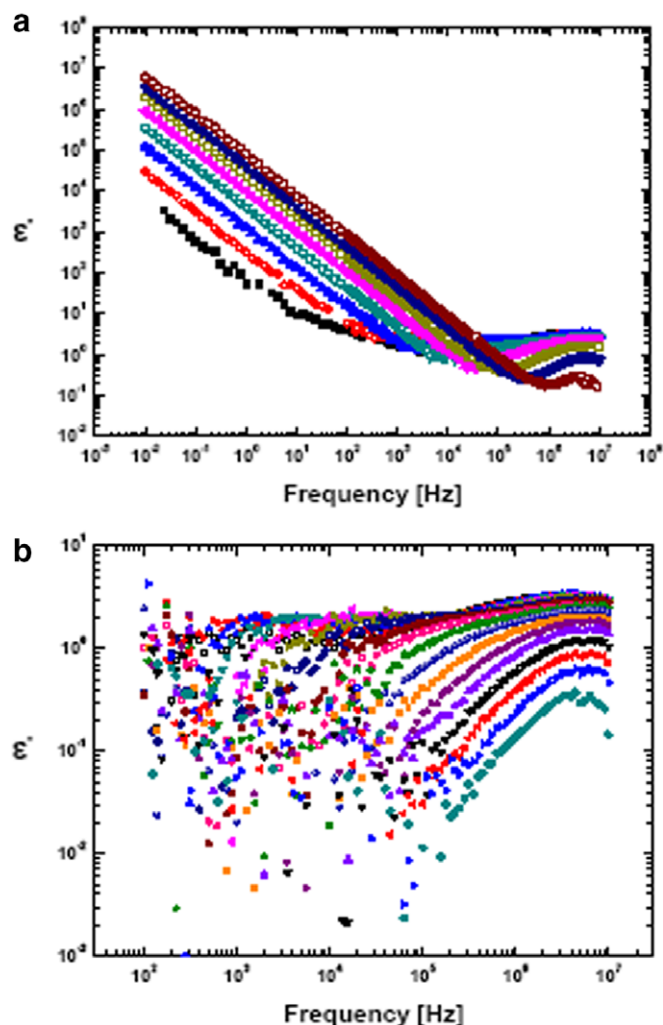


Fig. 7. $\varepsilon''(\omega)$ vs. frequency in trehalose/6% water at eight temperatures between 100 °C (top) and 30 °C (bottom), (b) $\varepsilon''(\omega)$ after subtraction of the dc conductivity.

sometimes well above the expected value of $b = 1$, presumably because of slow relaxation caused by diffusion of residual dust or crystallites. (We note that $C(\tau)$ is often expressed as $C(\tau) = 1 + a|g(t)|^2$ with $g(t) = \exp[-(t/\tau_\alpha)^\beta]$. Therefore the PCS correlation time τ in Eq. (4) is related to the usual structural relaxation time τ_α by $\tau_\alpha = 2^{1/\beta}\tau$.)

We carried out PCS experiments on many trehalose samples prepared using different methods as well as on several other sugars and sugar mixtures. Here we describe the results obtained with two trehalose/water samples prepared by the boiling method described earlier.

3.4.1. Sample 1: $T_B = 119.6$ °C; $C(H_2O) \sim 15\%$; predicted $T_G = 12 \pm 5$ °C

We collected between two and four PCS spectra for sample 1 at each of 14 temperatures between 298 and 383 K. As mentioned above, the PCS background level b , which ideally is $b = 1.0$, was sometimes larger than 1.0 because of residual dust or crystallites. In Fig. 9 we show

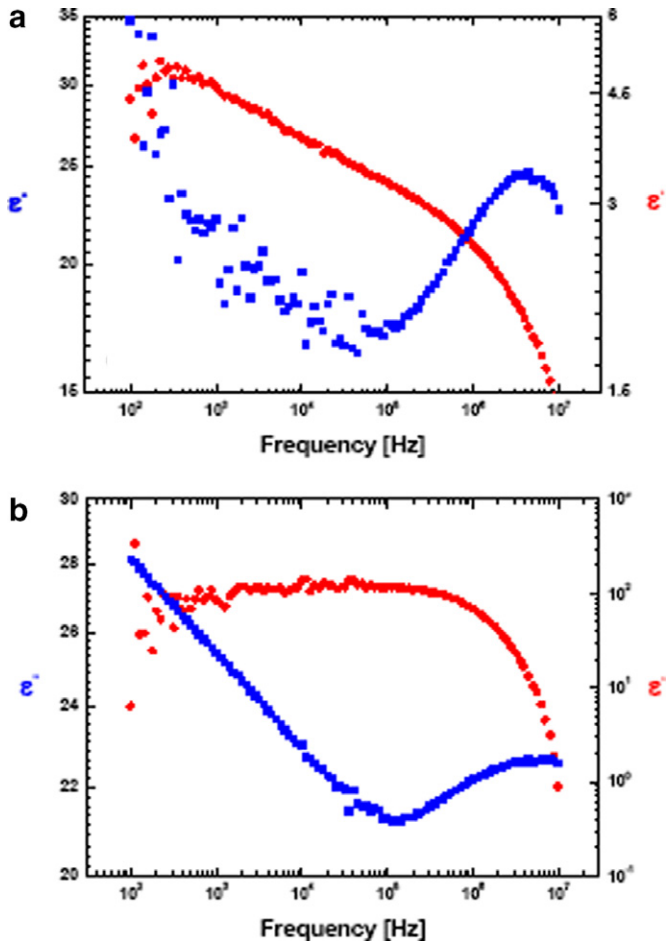


Fig. 8. Real and imaginary parts of $\epsilon(\omega)$ for the trehalose/6% water sample at (a) $T = 40\text{ }^\circ\text{C}$ and (b) $T = 80\text{ }^\circ\text{C}$.

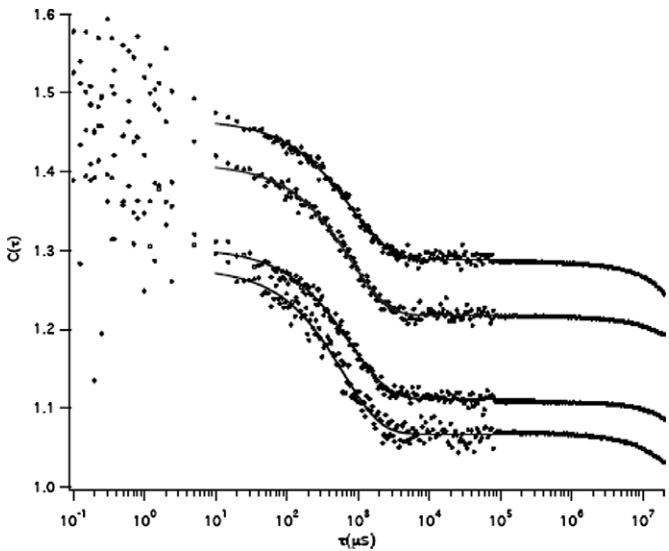


Fig. 9. Four successive PCS spectra of trehalose sample #1 at $T = 328\text{ K}$ showing the vertical shifts in the effective background level due to dust or crystallites. The solid lines are four-parameter KWW fits.

four consecutive PCS spectra at $T = 328\text{ K}$; the effective background levels range from 1.1 to 1.3. Nevertheless,

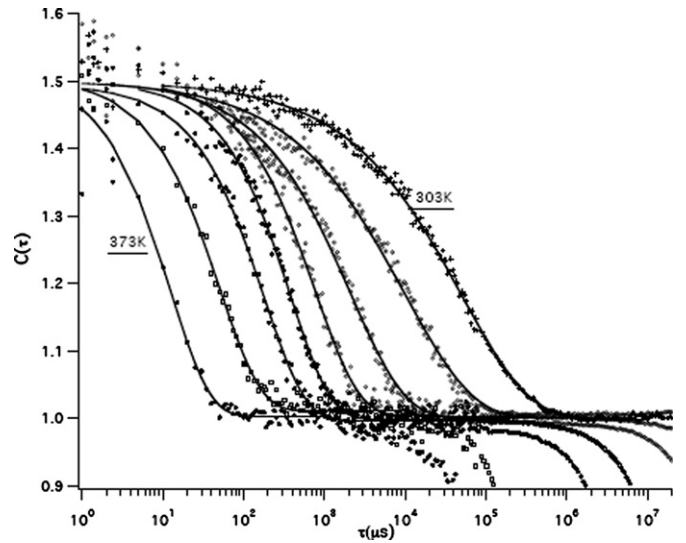


Fig. 10. PCS spectra of sample #1 with KWW fits at (right to left) $T = 303, 308, 318, 328, 338, 343, 363,$ and 373 K . The spectra and fits have been rescaled to make the baseline = 1.0 and the $t \rightarrow 0$ intercept = 1.5.

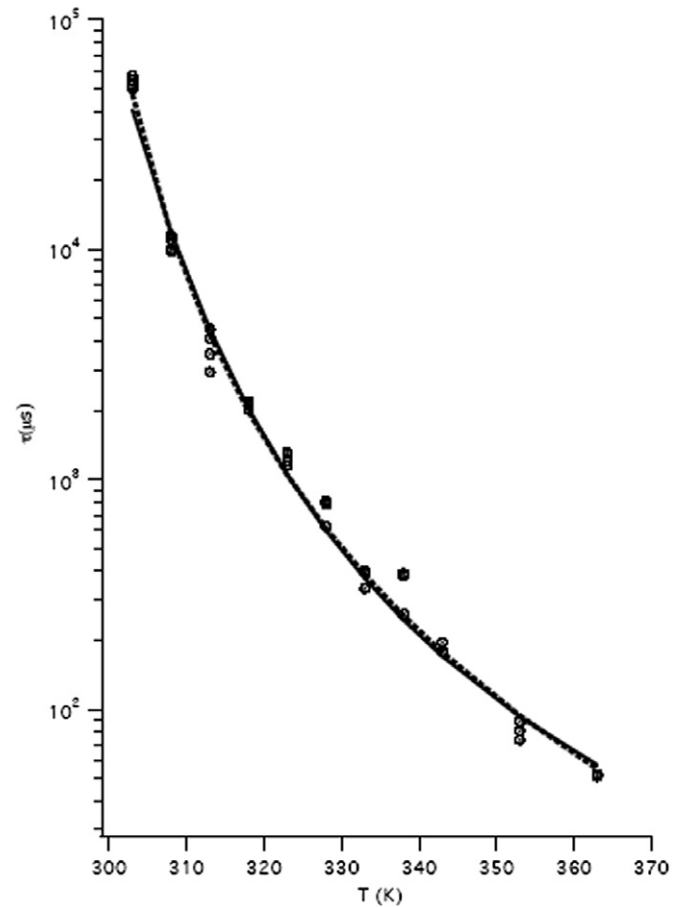


Fig. 11. τ values in μs from KWW fits to 37 PCS spectra of sample #1 with Vogel–Fulcher fit (solid line) and MCT power-law fit (broken line).

the values of τ and β extracted from the four-parameter KWW fits for these four spectra agree within $\pm 10\%$. (Note

that the excess background in these spectra does decay at long times since the particles producing the background diffuse). Of the 45 spectra analyzed, those for $T = 298, 373,$ and 383 K were found to give inconsistent values for τ and were not included in the subsequent analysis. (The reason for this inconsistency is not known.)

Fig. 10 shows PCS data of sample #1 with KWW fits for eight temperatures between 303 and 373 K. In this plot, the background levels have been shifted to $b = 1.0$ and the $t \rightarrow 0$ intercepts scaled to $b + a = 1.5$ to improve visibility. Finally, the 37 values of $\tau(T)$ obtained from the KWW fits for temperatures between 303 and 363 K were fit to a Vogel–Fulcher equation:

$$\tau_{VF}(\mu s) = \tau_0 \exp[A/(T - T_0)], \tag{5}$$

which gave $T_0 = 263 \pm 2$ K. The $\tau(T)$ data and VF fit are shown in Fig. 11. (Error bars for these fits were taken from the nonlinear confidence limits returned by the fitting program). The glass transition temperature T_G , obtained by extrapolating τ_{VF} to 1000 s, is $T_G = 284 \pm 2$ K = 11 ± 2 °C, in close agreement with the predicted $T_G = 12 \pm 5$ °C.

3.4.2. Sample 2: $T_B = 126$ °C; $C(H_2O) \sim 9\%$; predicted $T_G = 30 \pm 5$ °C

PCS spectra for sample 2 were collected at 20 temperatures between 298 and 353 K. Good four-parameter KWW fits were obtained for 24 spectra in the range 311–340 K. In Fig. 12 we show four PCS spectra with the corresponding KWW fits. The spectra and fits have been rescaled, as for sample 1, to make the background $b = 1.0$ and the $t \rightarrow 0$ intercepts = 1.5. The values of τ determined in the KWW fits are plotted in Fig. 13. Again, we show fits of $\tau(T)$ to the Vogel–Fulcher equation (5) which gave $T_0 = 293 \pm 2$ K. Extrapolating the VF fit to $\tau_{VF} = 1000$ s, we find $T_G = 309 \pm 2$ K = 36 ± 2 °C, in reasonable agreement with the predicted $T_G = 30 \pm 5$ °C.

3.5. Viscosity

Dynamic rheology measurements were performed with an ARES rheometer (TA Instruments) using 25 mm parallel plates. Measurements were carried out in the dynamic mode at 1 rad/s, with strain = 1%. Several temperature scans were carried out in which the temperature was kept below the boiling temperature used in preparing the trehalose sample. In these experiments, the viscosity generally

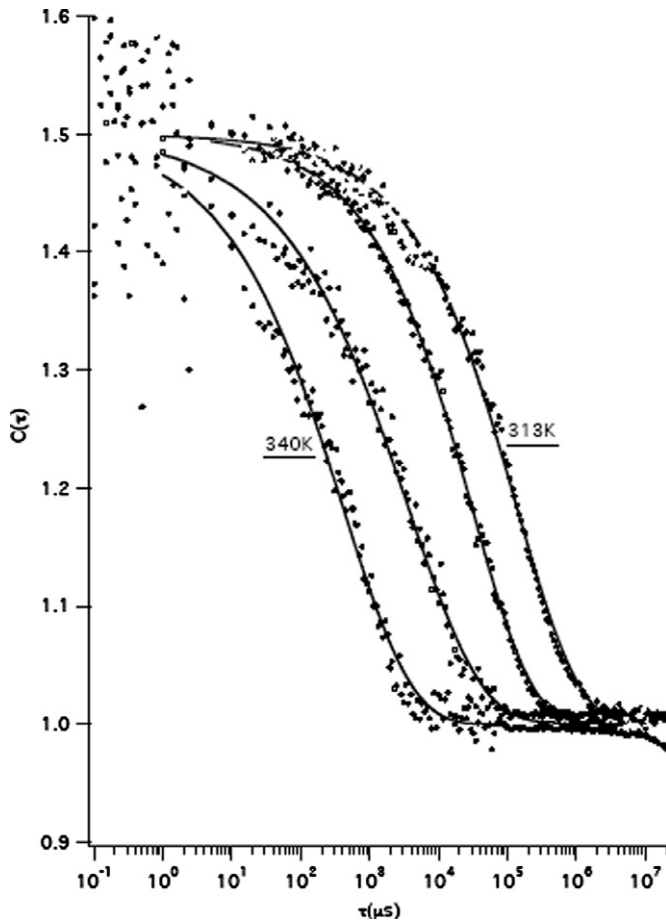


Fig. 12. PCS spectra of sample #2 with KWW fits at (right to left) $T = 313, 317, 323,$ and 340 K. The spectra and fits were rescaled as described in Fig. 10.

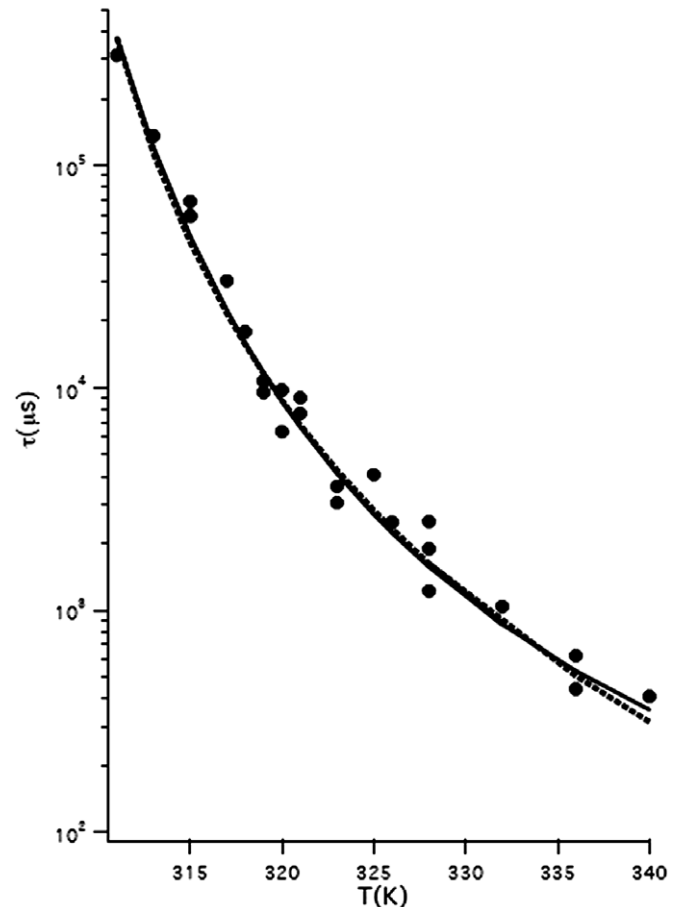


Fig. 13. τ values in μs from KWW fits to 24 PCS spectra of sample #2 with Vogel–Fulcher fit (solid line) and MCT power-law fit (broken line).

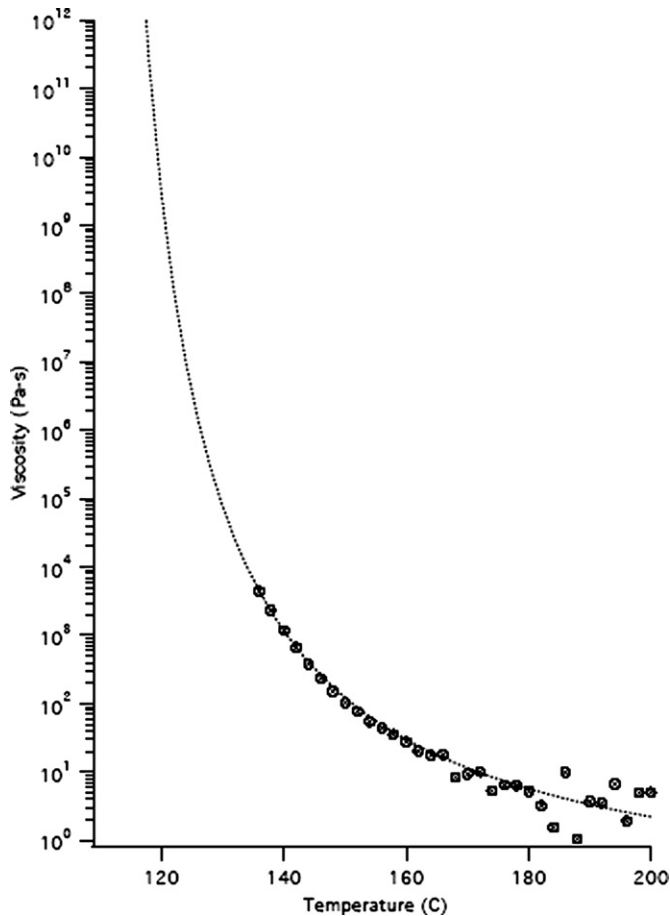


Fig. 14. Viscosity of trehalose sample after heating to 200 °C. Dynamic measurement at 1 rad/s with 25 mm diam parallel plates; strain = 1%. Symbols are experimental data. Solid line is the Vogel–Fulcher fit: $\eta = 0.0687 \exp[323.5/(T - 106.8)]$ (Pa-s). Extrapolated $T_G = 117.5$ °C ($\eta = 1 * 10^{12}$ Pa-s).

increased with time, presumably because of slow water evaporation through the open sides of the rheometer cell causing the residual water concentration to decrease and T_G to increase.

In one experiment, after loading the sample cell with a sample prepared with an initial water concentration of ~5% and predicted $T_G \sim 55$ °C, the temperature was increased to 200 °C before beginning a temperature scan. The resulting viscosity data is shown in Fig. 14, together with a Vogel Fulcher fit. Extrapolating the fit to $\eta = 1 * 10^{12}$ Pa-s indicates $T_G \sim 117$ °C, close to the value $T_G = 114$ °C for anhydrous trehalose reported by Crowe et al. [17], indicating that heating the sample to 200 °C is apparently sufficient to remove all residual water. The data shown in Fig. 14 is therefore assumed to represent the temperature-dependent viscosity of anhydrous trehalose.

4. Discussion

The relaxation dynamics of molecular liquids cooled towards the glass transition exhibit complex behavior ending in the α -relaxation. Data on these materials has often

been analyzed by fitting to the predictions of the Mode Coupling Theory (MCT). MCT predicts that the correlation (or relaxation) function $\phi(t)$ follows a two-step relaxation scenario ending in the final α -relaxation process described by the stretched-exponential KWW function [37,38]. The α -relaxation process is preceded by two power law regions: the critical decay t^{-a} towards a plateau at f_Q , and the von Schweidler decay $-t^b$ away from the plateau that leads into the final α -decay.

Exploration of the full relaxation process requires probing a broad range of times (or frequencies) which has been carried out with a number of different techniques. PCS experiments alone cannot provide a sufficient range of times since the early part of the relaxation occurs at times too short to appear in the PCS data. An exception is colloidal glasses where the time scale is much longer so that the full relaxation process *can* be probed using PCS and compared in detail to MCT predictions, as illustrated by the work of van Meegen and coworkers [39].

Since our experiments only probe the α -relaxation region and have not explored the region of the two power laws (the β -relaxation region), we cannot establish the applicability of MCT to the trehalose–water system. However, if we assume that MCT is applicable, we can obtain a preliminary estimate of relevant MCT parameters. First, we recall that early estimates of the MCT crossover temperature T_c were obtained from fits of viscosity data to the MCT prediction for the viscosity: $\eta = \eta_0(T - T_c)^{-\gamma}$ as shown, e.g., in Fig. 4.25 of Götze’s 1989 Les Houches lecture [40] or Fig. 16 of Ref. [41]. Similarly, the α -relaxation time τ_α , which we have measured in our PCS experiments, is predicted by MCT to have the temperature dependence:

$$\tau_\alpha = \tau_0(T - T_c)^{-\gamma}. \quad (6)$$

Fits of the $\tau(T)$ values for samples #1 and 2 shown in Figs. 11 and 13 to Eq. (6), which are included in the figures, gave estimates of T_c for these two samples as

$$\text{Sample 1 : } T_c = 293 \pm 1 \text{ K} (\sim T_G + 11 \text{ K}),$$

$$\text{Sample 2 : } T_c = 305.5 \pm 1 \text{ K} (\sim T_G + 2 \text{ K}).$$

Second, rough estimates of the MCT exponents a and b can also be obtained from these fits since the exponent γ in Eq. (6) is related to the MCT exponents a and b by

$$\gamma = 1/2a + 1/2b, \quad (7)$$

while a and b are related to each other by the MCT relation

$$F^2(1 - a)/\Gamma(1 - 2a) = F^2(1 + b)/\Gamma(1 + 2b) = \lambda, \quad (8)$$

where λ is the MCT exponent parameter and $\Gamma(x)$ is the Gamma function. Consequently, a and b can be estimated from γ . Götze has tabulated pairs of values for a and b that satisfy Eq. (8) [38]. Using these values, we computed and plotted γ vs. a . Using linear interpolation, the values of a and λ corresponding to the PCS results for γ for the two samples are

Sample 1 : $\gamma = 3.476, a = 0.237, \lambda = 0.865,$

Sample 2 : $\gamma = 3.817, a = 0.22, \lambda = 0.887.$

For comparison, the values of a for two well-studied molecular glassformers, propylene carbonate and salol, are 0.29 and 0.327, respectively.

Again, we stress that, in view of the limited time range covered by our experiments this analysis is only intended to provide preliminary estimates for the MCT crossover temperature T_c and critical exponent a . We anticipate that future experiments will provide more definitive tests of the applicability of MCT to this system.

Finally, we note that it is possible to estimate the activation energy Δh^* from the PCS results and compare with the value of 33.9 kcal/mol. found from the DSC measurements in Section 3.2. If we assume that close to T_G $\tau(T)$ follows the Arrhenius law $\tau = \tau_0 \exp(\Delta h^*/RT)$, then the limiting slope close to T_G of $\ln(\tau)$ vs. $1/T$ would be $\Delta h^*/R$. From the VF fit to the data of sample #1 shown in Fig. 11, we found the slope to be 22,771 from which we estimate $\Delta h^* = 45.2$ kcal/mol. in reasonable agreement with the DSC value.

5. Conclusions

The dynamical properties of trehalose/water solutions have been explored with a range of experimental techniques. Several typical signatures of the glass transition were observed:

1. A break in the slope of the Brillouin shift vs. temperature curve.
2. A step in the specific heat curve.
3. An α -relaxation time that follows the Vogel–Fulcher equation and can also be described by an MCT power-law equation which indicates that $T_c \sim T_G + 11$ K.
4. Viscosity that increases rapidly with decreasing temperature, that can be described by a Vogel–Fulcher equation.

Dielectric spectroscopy has not yet provided useful information on the α -relaxation dynamics because the low-frequency dielectric loss is apparently dominated by dc conductivity of unknown origin. However, evidence of temperature-dependent secondary relaxation at higher frequencies has been observed.

In view of the importance of sugars (including trehalose) in biology, biotechnology, and the food industry, further experiments along these lines are clearly worth pursuing.

Acknowledgements

We thank Harry Levine for helpful discussions and for suggesting trehalose as an interesting sugar for study, and Cargill, Inc for providing the trehalose dihydrate used in

these experiments. We also thank Marilyn Gunner and Lisa Lapidus for helpful discussions about handling Trehalose, and Wolfgang Gotze for helpful suggestions on this manuscript. This US–Korea Cooperative Research Project is supported by the US National Science Foundation under grant NSF-INT 0216824 and by the Korea Science and Engineering Foundation (KOSEF) through grant F01-2003-000-00024-0. Research in New York was supported by the NSF under grant DMR-0243471.

References

- [1] NIST, NIST Chemistry Webbook Available from: <http://webbook.nist.gov/chemistry>.
- [2] L. Slade, H. Levine, Critical Rev. Food Sci. Nutr. 30 (1991) 115.
- [3] L. Slade, H. Levine, Adv. Food Nutr. Res. 38 (1995) 103.
- [4] J.M.V. Blanshard, P.J. Lillford, The Glassy State in Foods, Nottingham University Press, 1993.
- [5] S.P. Ding, J. Fan, J.L. Green, Q. Lu, E. Sanchez, C.A. Angell, J. Therm. Anal. 47 (1996) 1391.
- [6] K.L. Koster, Y.P. Lei, M. Amderson, S. Martin, G. Bryant, Biophys. J. 78 (2000) 1932.
- [7] C. Macdonald, G.P. Johari, J. Mol. Struct. 523 (2000) 119.
- [8] P.D. Orford, R. Parker, S.G. Ring, Carbohydrate Res. 196 (1990) 11.
- [9] J.L. Green, C.A. Angell, J. Phys. Chem. 93 (1989) 2880.
- [10] A.D. Elbein, Y.T. Pan, I. Pastuszak, D. Carroll, Glycobiology 13 (2003) 17R.
- [11] J.H. Crowe, F.A. Hoekstra, L.M. Crowe, Annu. Rev. Physiol. 54 (1992) 579.
- [12] J.H. Crowe, J.F. Carpenter, L.M. Crowe, Annu. Rev. Physiol. 60 (1998) 73.
- [13] J. Buitink, O. Leprince, Cryobiology 48 (2004) 215.
- [14] R. Mouradian, C. Womersley, J.M. Crowe, J.H. Crowe, Biochim. Biophys. Acta 778 (1984) 615.
- [15] L.M. Crowe, R. Mouradian, J.H. Crowe, S.A. Jackson, C. Womersley, Biochim. Biophys. Acta 769 (1984) 141.
- [16] J.F. Carpenter, L.M. Crowe, J.H. Crowe, Biophys. Biochim. Acta 923 (1987) 109.
- [17] L.M. Crowe, D.S. Reid, J.H. Crowe, Biophys. J. 71 (1996) 2087.
- [18] J.V. Ricker, N.M. Tsvetkova, W.F. Wolkers, C. Leidy, F. Tablin, M. Longo, J.H. Crowe, Biophys. J. 84 (2003) 3045.
- [19] T. Chen, Cryobiology 40 (2000) 277.
- [20] S.J. Hagen, J. Hofrichter, W.A. Eaton, Science 269 (1995) 959.
- [21] M.T. Cicerone, C.L. Soles, Biophys. J. 86 (2004) 3836.
- [22] T.E. Dirama, G.A. Carri, A.P. Sokolov, J. Chem. Phys. 122 (2005) 114505.
- [23] G. Caliskan, D. Mechtani, J.H. Roh, A. Kisliuk, A.P. Sokolov, S. Azzam, M.T. Cicerone, S. Lin-Gibson, I. Peral, J. Chem. Phys. 121 (2004) 1978.
- [24] A. Lerbret, P. Bordat, F. Affouard, M. Descamps, F. Migliardo, J. Phys. Chem. B 109 (2005) 11046.
- [25] H. Levine, L. Slade, BioPharm. 5 (1992) 36.
- [26] Exploratorium, Available from: <http://www.exploratorium.edu/cooking/candy/>.
- [27] A. Patist, H. Zoerb, Colloids Surf. B 40 (2005) 107.
- [28] G.R. Moran, K.R. Jeffrey, J.M. Thomas, J.R. Stevens, Carbohydrate Res. 328 (2000) 573; J. Oh, J.-A. Seo, H.K. Kim, Y.-H. Hwang, in preparation.
- [29] J.-A. Seo, S.J. Kim, J. Oh, H.K. Kim, Y.-H. Hwang, J. Korean Phys. Soc. 44 (2004) 523.
- [30] S. Magazu, G. Maisano, D. Majolino, P. Migliardo, A.M. Musolino, V. Villari, Prog. Theor. Phys. – Supplement 126 (1997) 195.
- [31] F. Migliardo, V. Magazu, M. Migliardo, J. Mol. Liquids 110 (2004) 11.
- [32] C. Branca, S. Magazu, G. Maisano, P. Migliardo, J. Chem. Phys. 111 (1999) 281.

- [33] A. De Gusseme, L. Carpentier, J.F. Willart, M. Descamps, *J. Phys. Chem. B* 107 (2003) 10879;
D.L. French, T. Arakawa, T. Li, *Biopolymers* 73 (2004) 524.
- [34] D.P. Miller, J.J.d. Pablo, H. Corti, *Pharm. Res.* 14 (1997) 578.
- [35] C.S. Pereira, R.D. Lins, I. Chandrasekhar, L.C.G. Freitas, P.H. Hunenberger, *Biophys. J.* 86 (2004) 2273.
- [36] C.T. Moynihan, A.J. Easteal, J. Wilder, J. Tucker, *J. Phys. Chem.* 78 (1974) 2673.
- [37] W. Götze, L. Sjögren, *Rep. Prog. Phys.* 55 (1992) 241.
- [38] W. Götze, *J. Phys. Condens. Matter* 2 (1990) 8485.
- [39] W. van Meegen, S.M. Underwood, *Phys. Rev. E* 49 (1994) 4206.
- [40] W. Götze, in: J.P. Hansen, D. Levesque, J. Zinn-Justin (Eds.), *Liquids Freezing and the Glass Transition – Les Houches LI 1989*, North Holland, 1991, p. 292.
- [41] G. Li, W.M. Du, A. Sakai, H.Z. Cummins, *Phys. Rev. A* 46 (1992) 3343.